



Molecular Crystals and Liquid Crystals Science and Technology. Section A. Molecular Crystals and Liquid Crystals

Publication details, including instructions for authors and
subscription information:

<http://www.tandfonline.com/loi/gmcl19>

Non-Linear Theory of Flexoelectrically Induced Periodic Distortions in Nematic Liquid Crystals

Alberto Cama^a, Paolo Galatola^a, Claudio Oldano^a & Mauro Rajteri^a

^a Dipartimento di Fisica, Politecnico di Torino, Corso Duca degli
Abruzzi 24, 10129, Torino, Italy

Version of record first published: 23 Sep 2006.

To cite this article: Alberto Cama, Paolo Galatola, Claudio Oldano & Mauro Rajteri (1995): Non-Linear Theory of Flexoelectrically Induced Periodic Distortions in Nematic Liquid Crystals, Molecular Crystals and Liquid Crystals Science and Technology. Section A. Molecular Crystals and Liquid Crystals, 261:1, 177-185

To link to this article: <http://dx.doi.org/10.1080/10587259508033464>

PLEASE SCROLL DOWN FOR ARTICLE

Full terms and conditions of use: <http://www.tandfonline.com/page/terms-and-conditions>

This article may be used for research, teaching, and private study purposes. Any substantial or systematic reproduction, redistribution, reselling, loan, sub-licensing, systematic supply, or distribution in any form to anyone is expressly forbidden.

The publisher does not give any warranty express or implied or make any representation that the contents will be complete or accurate or up to date. The accuracy of any instructions, formulae, and drug doses should be independently verified with primary sources. The publisher shall not be liable for any loss, actions, claims, proceedings, demand, or costs or damages whatsoever or howsoever caused arising directly or indirectly in connection with or arising out of the use of this material.

NON-LINEAR THEORY OF FLEXOELECTRICALLY INDUCED PERIODIC DISTORTIONS IN NEMATIC LIQUID CRYSTALS

ALBERTO CAMA, PAOLO GALATOLA, CLAUDIO OLDANO AND MAURO RAJTERI

Dipartimento di Fisica, Politecnico di Torino, Corso Duca degli Abruzzi 24,
 10129 Torino, Italy

Abstract The peak intensities of the diffraction grating obtained in a nematic liquid crystal cell above the critical point of the flexoelectrically induced Pikin transition have been measured as a function of the applied voltage. The obtained results have been analyzed in the framework of a non-linear theory of the transition.

INTRODUCTION

It is well known that many liquid crystals (LC) give rise to periodically modulated structures behaving as diffraction gratings. The most interesting cases involve the N^* and S_c^* LC with helix axis perpendicular to the boundary planes, and the field-induced periodic distortion in nematic LC (NLC) found by R. B. Mayer^{1,2} and S. A. Pikin^{3,4,5}. All these gratings display an unusual and interesting behavior of the polarization properties of the diffracted beams. They have been theoretically considered in a series of papers^{6,7,8}. An experimental check of the above theory has been recently published for the S_c^* LC⁹.

The aim of this paper is to compare theory and experiment for the Pikin-type gratings, which are obtained by applying a d.c. electric field to a planar NLC cell. Above a threshold value of the field a Fréedericksz-type second order transition is obtained, which can be either periodic or aperiodic depending on the elastic, dielectric and flexoelectric properties of the NLC. A phase diagram for the appearance of the different types of distorted structures has recently been published¹⁰. The Pikin-type distortion is

induced by flexoelectricity in NLC with a dielectric anisotropy small enough, and give rise to a diffraction grating whose wavevector is parallel to the boundary planes and orthogonal to the undistorted director. This grating has received some attention in the last decade in view of the possible applications^{11,12} owing to the fact that it displays unusual and interesting polarization properties and that the grating efficiencies of the different peaks can be easily modulated by the electric field. Moreover, the analysis of the diffracted peaks intensities is a powerful method to measure the flexoelectric and elastic constants of the material.

The interpretation of the experimental data requires two separate steps: the computation of the distortion and the solution of the optical problem. For the second problem, exact numerical solutions have already been developed^{13,8}. The first step requires the minimization of the free energy of the system. A linear theory is generally used^{3,4,10}, which only allows one to compute the threshold field and the shape (twist-splay ratio) of the initial distortion just above the threshold. The study of the distortion amplitude as a function of the applied field requires a non linear theory. Such a theory has been developed by Pikin^{5,14} in the particular case of equal elastic constants, zero dielectric anisotropy and short wavelength limit. In order to fit the experimental data, we have developed a more general non-linear theory.

THEORY

The free energy density of a NLC in an external electric field \underline{E} is given by⁵

$$F = \frac{1}{2}K_1(\nabla \cdot \hat{n})^2 + \frac{1}{2}K_2(\hat{n} \cdot \nabla \times \hat{n})^2 + \frac{1}{2}K_3(\hat{n} \times \nabla \times \hat{n})^2 - e_1(\nabla \cdot \hat{n})(\underline{E} \cdot \hat{n}) + e_3 \underline{E} \cdot (\hat{n} \cdot \nabla) \hat{n} - \frac{1}{2}\epsilon_o \epsilon_{\perp} E^2 - \frac{1}{2}\epsilon_o \epsilon_a (\underline{E} \cdot \hat{n})^2 \quad (1)$$

where K_i ($i=1,2,3$) are the elastic constants, e_1 , e_3 are the flexoelectric coefficient and ϵ_a is the dielectric anisotropy. We assume strong planar anchoring conditions $\hat{n} = \hat{x}$ at the cell boundary planes $z = \pm d/2$. The electric field \underline{E} is along \hat{z} . The director profile above threshold is assumed as

$$\begin{aligned}\eta(y, z) &= \sum_{n=1}^{\infty} \cos(nQ_y y) \eta_n(z) \\ \varphi(y, z) &= \sum_{n=1}^{\infty} \sin(nQ_y y) \varphi_n(z)\end{aligned}\quad (2)$$

where $\vartheta = \pi/2 - \eta$ and φ are the polar angles of the director. $Q_y = \pi q/d$ is the wavevector of the periodic profile. Eq. (2) is a generalization of the profile found in the linear analysis for small distortions, in which only the first harmonic in y is nonzero. Due to the boundary conditions, we can write

$$\begin{aligned}\eta_n(z) &= \eta_{n1} \cos\left(\frac{\pi}{d}z\right) + \eta_{n2} \sin\left(2\frac{\pi}{d}z\right) + \eta_{n3} \cos\left(3\frac{\pi}{d}z\right) + \dots \\ \varphi_n(z) &= \varphi_{n1} \cos\left(\frac{\pi}{d}z\right) + \varphi_{n2} \sin\left(2\frac{\pi}{d}z\right) + \varphi_{n3} \cos\left(3\frac{\pi}{d}z\right) + \dots\end{aligned}\quad (3)$$

Using these expressions, the average free energy per unit surface [in the (x,y)-plane] \mathfrak{F} can be expressed as a function of the various Fourier components according to

$$\mathfrak{F} = \frac{\pi^2 K_1}{2d} f(\eta_{ij}, \varphi_{ij}, q; v, r, s, \text{sgn}(\epsilon_a), e) \quad (4)$$

where we have introduced the normalized parameters

$$r = \frac{K_2}{K_1} \quad s = \frac{K_3}{K_1} \quad q = \frac{d}{\pi} Q_y \quad e = \frac{e_1 - e_3}{\sqrt{\epsilon_o |\epsilon_a|} K_1} \quad v = \frac{1}{\pi} \sqrt{\frac{\epsilon_o |\epsilon_a|}{K_1}} E d \quad (5)$$

The stable director configuration corresponds to the minimum of the function f with respect to $\eta_{ij}, \varphi_{ij}, q$. The minimization has been done by first expanding f in a power series of the parameters η_{ij}, φ_{ij} , which are identically equal to zero below the transition point and monotonically increase with the field above this point. The search of the minimum is straightforwardly done by using the steepest descent method. The only difficulty comes from the fact that the number of terms appearing in the free-energy expression dramatically increase by increasing the number of Fourier components and the order of the power expansion. We give here the terms up to sixth order in η_{11}, φ_{11} , obtained by retaining only one Fourier component in Eq. (2) and (3), and neglecting the terms which depend on the field gradient:

$$\begin{aligned}
\mathfrak{S} = & \frac{1}{4}\varphi_{11}^2q^2 - \frac{3}{64}\varphi_{11}^4q^2 + \frac{5}{768}\varphi_{11}^6q^2 + \frac{1}{4}\varphi_{11}^2r + \frac{3}{64}\varphi_{11}^4q^2s - \frac{5}{768}\varphi_{11}^6q^2s + \\
& + \frac{1}{4}\eta_{11}^2 - \frac{3}{64}\eta_{11}^2\varphi_{11}^2q^2 - \frac{5}{768}\eta_{11}^2\varphi_{11}^4q^2 + \frac{1}{32}\eta_{11}^2\varphi_{11}^2r + \frac{1}{4}\eta_{11}^2q^2r + \\
& - \frac{15}{64}\eta_{11}^2\varphi_{11}^2q^2r + \frac{5}{64}\eta_{11}^2\varphi_{11}^4q^2r + \frac{1}{64}\eta_{11}^2\varphi_{11}^2s + \frac{9}{64}\eta_{11}^2\varphi_{11}^2q^2s + \\
& - \frac{55}{768}\eta_{11}^2\varphi_{11}^4q^2s - \frac{3}{64}\eta_{11}^4 + \frac{4}{192}\eta_{11}^4\varphi_{11}^2q^2 + \frac{5}{768}\eta_{11}^4\varphi_{11}^2r + \\
& + \frac{5}{192}\eta_{11}^4\varphi_{11}^2q^2r + \frac{3}{64}\eta_{11}^4s - \frac{1}{192}\eta_{11}^4\varphi_{11}^2s - \frac{5}{256}\eta_{11}^4\varphi_{11}^2q^2s + \\
& + \frac{5}{768}\eta_{11}^6 - \frac{5}{768}\eta_{11}^6s - \frac{1}{2}\eta_{11}\varphi_{11}qev + \frac{3}{64}\eta_{11}\varphi_{11}^3qev + \\
& - \frac{5}{3072}\eta_{11}\varphi_{11}^5qev + \frac{3}{32}\eta_{11}^3\varphi_{11}qev - \frac{5}{768}\eta_{11}^3\varphi_{11}^3qev - \frac{5}{384}\eta_{11}^5\varphi_{11}qev + \\
& - \frac{1}{4}\eta_{11}^2v^2\operatorname{sgn}(\varepsilon_a) + \frac{3}{64}\eta_{11}^4v^2\operatorname{sgn}(\varepsilon_a) - \frac{5}{1152}\eta_{11}^6v^2\operatorname{sgn}(\varepsilon_a)
\end{aligned}
\tag{6}$$

In order to avoid unpracticable computations, drastic approximations are needed. As a matter of fact, our experimental results are fitted quite well, in the whole range of the applied tension, by only retaining terms up to the sixth order in the parameters $\eta_{11}, \varphi_{11}, \eta_{12}, \varphi_{12}$ and of the second order in q , and neglecting the terms in the field gradient. More generally, our theoretical analysis has shown that the higher-order Fourier components in the y direction are typically at least one order of magnitude smaller than the same order components in the z direction. On the other hand, the terms in the field gradient, which cannot be treated in practice to the higher-power orders owing to their complexity¹⁰, are generally non-negligible for arbitrary direction of the wavevector \underline{q} . However we have found that their role drastically decreases by decreasing the component of \underline{q} in the direction of the undistorted director. This explains the fact that a good fit has been obtained in the absence of such terms, since in our experiment the wave-vector is orthogonal to the undistorted director.

EXPERIMENTAL AND RESULTS

A NLC with small dielectric anisotropy and strong flexoelectric coupling with the electric field¹⁰ is needed in order to obtain a Pikin type periodic structure. We have used the NLC NP1052 (Merck), which is a binary eutectic of aromatic esters.

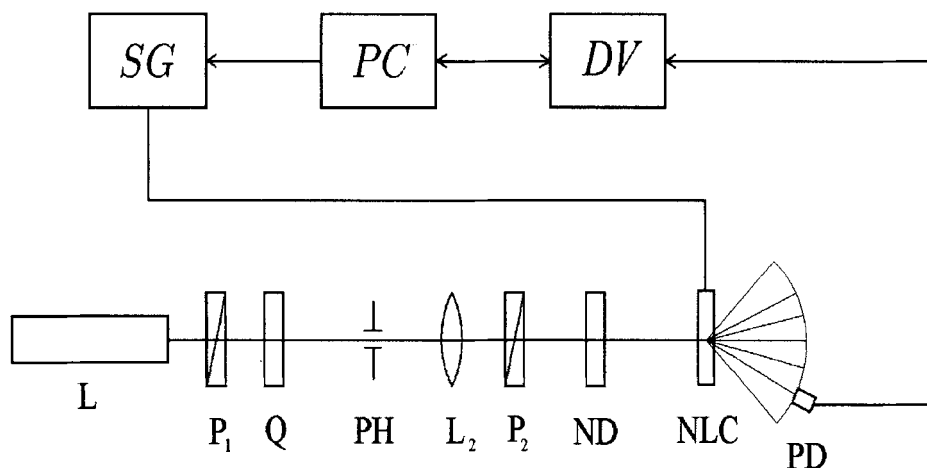


FIGURE 1 Experimental set-up. L: 10 mW H_e-N_e laser; P_1 , P_2 : polarizers; Q: quarter-wave plate; PH: pinhole; L_2 : converging lens; ND: neutral density filters; NLC: nematic liquid crystal cell; PD: analyzer and photodiode; SG: signal generator; PC: personal computer; DV: digital voltmeter.

This compound is nematic in the range $15 \div 48^\circ C$ with dielectric constants $\epsilon_{||} = 5.9$, $\epsilon_{\perp} = 5.8$ (1 kHz), refractive indexes $n_e = 1.701$, $n_o = 1.561$, and resistivity $> 10^{10} \Omega \cdot cm$ at $20^\circ C$. The planar cell has been obtained by coating the glasses with a thin conductive layer of ITO and SiO_x evaporated at an angle of 60° degrees from the normal, and using mylar spacers of thickness $d \approx 10 \mu m$. A d.c. voltage is applied to the sample because the flexoelectric coupling with the electric field is linear. The experimental setup is reported in Fig. 1. The polarizer P_1 and the $\lambda/4$ wave plate act as an optical isolator of the light emitted by the laser and produce a circular polarized beam, which is filtered by the pinhole and focused on the sample by the converging lens. The polarization states of the incoming and outgoing light are selected by the polarizer P_2 and by an analyzer. The intensity of the diffracted peaks is measured using a photodiode with an area of $1 cm^2$ to collect all the scattered light, that for the higher orders is rather broad. The photographs of the diffracted peaks are reported in Fig. 2. One may notice that only even order peaks appear for EE polarization states and only odd orders peaks for EO polarization states. The same "selection rule" is valid for OO (odd orders only) and OE (even orders only) polarization states. The main difference lies in the fact that the intensities of the diffracted beams for OO polarizations are smaller than for EE polarizations.



FIGURE 2 Photographs of the diffraction pattern at $V=5.2$ V at normally incident light for different polarization states. Here E and O denote extraordinary and ordinary beams, respectively, in the undistorted NLC. The first and second symbols refer to incident and diffracted beams.

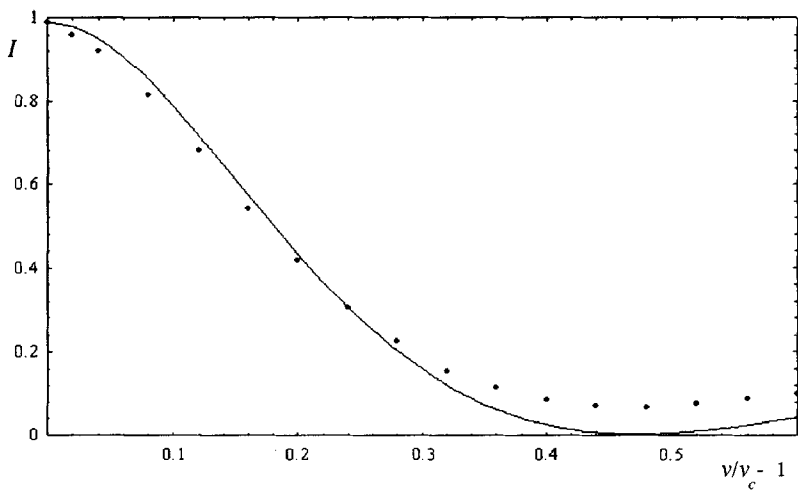


FIGURE 3 Zeroth order relative intensity (grating efficiency) for EE polarizations.

The experimental grating efficiencies (ratios between the intensities of the diffracted beams and of the input beam within the glasses; the effect of the multiple reflections at the external boundary of the glasses is within the experimental errors) and the theoretical fits are reported in Figs. 3-6 as a function of $v/v_c - 1$, where v_c is the threshold voltage. Zeroth order efficiencies for OO polarizations is very close to unity, the difference being

of the order of the experimental errors. The best-fit parameters are: $v_c = 5$ V, $d=8.25$ μm , $\epsilon_a=0.267$, $e=1.293$, $r=0.798$, $s=2$.

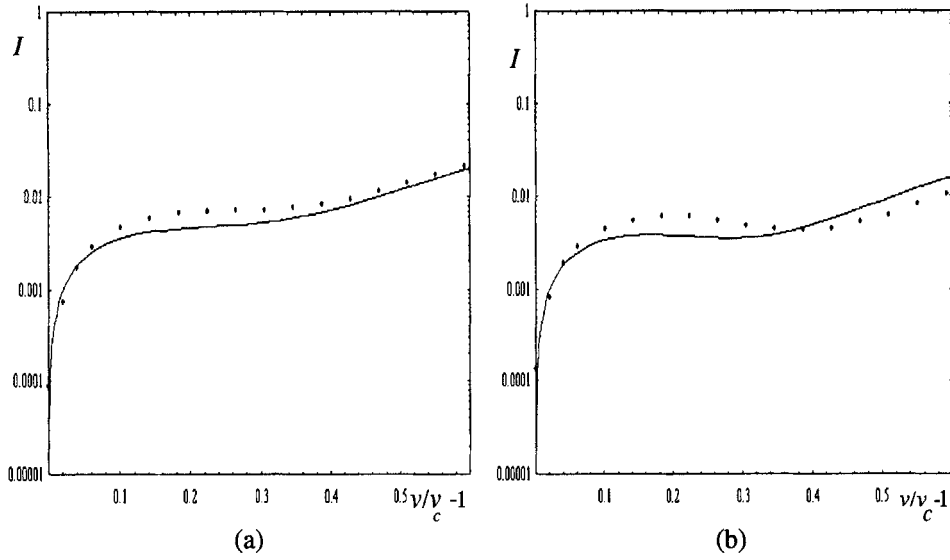


FIGURE 4 First order for EO (a) and OE (b) grating efficiencies.

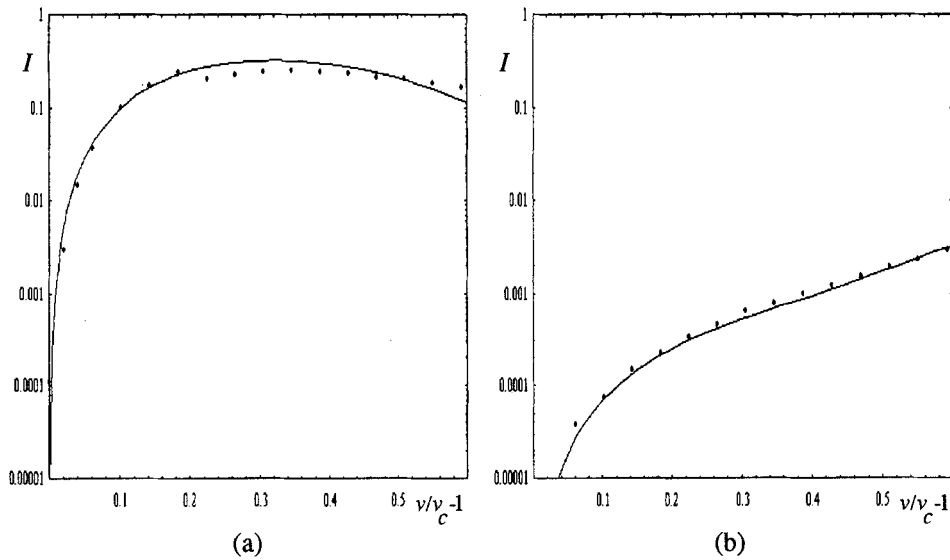


FIGURE 5 Second order for EE (a) and OO (b) grating efficiencies.

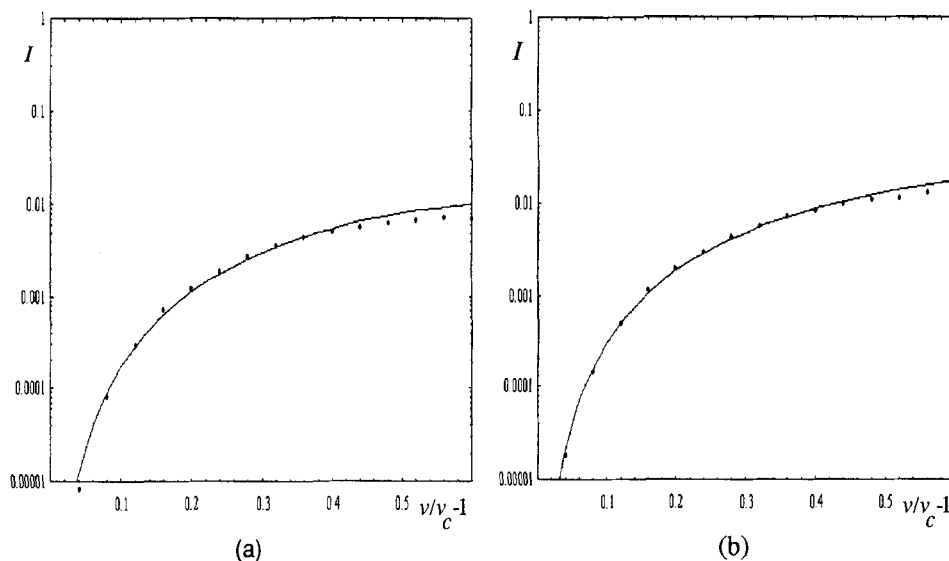


FIGURE 6 Third order for EO (a) and OE (b) grating efficiencies.

CONCLUSIONS

The analysis of the intensities of the beams diffracted by an anisotropic NLC grating is a complicated task, since it requires the simultaneous determination of the three-dimensional profile of the director field, and the solution of the optical problem. Therefore, approximate techniques and simpler limiting cases are usually considered. Here we have developed a nonlinear numerical approach providing an exact solution to the problem, without making additional unphysical approximations. The agreement between the experimental data and the numerical model is good and allows one to determine some of the material's physical constants.

The striking features of this type of gratings are the "selection rules" which are valid at any incidence angle if the grating wavevector is parallel to the incidence plane, thus giving rise to diffracted beams in the same plane. They can be summarized as follow. An input beam linearly polarized in the incidence plane gives rise to even order peaks polarized in the same plane and to odd order peaks with the opposite polarization. Similar properties are found for the orthogonal polarization state of the incident beam, as explained in the preceding section. A similar behavior is not fully surprising if one considers the polarization properties of the light scattered by the thermal fluctuations of the director (as evident the distortion above the critical point can be considered as a huge

amplifications of the critical fluctuations). It is in fact well known that in our scattering geometry the thermal fluctuations only give depolarized scattered light. This means that only the EO and OE scattering amplitudes are different from zero¹⁵. By increasing the distortion amplitudes this property of the diffracted beams is conserved, giving rise to the first order peaks. If we assume that the second order peaks are generated by the first order ones (and so on), we can fully explain the selection rules. We emphasize the fact that the peaks which are forbidden by our selection rules are strictly forbidden, in the sense that the theory gives intensities exactly equal to zero, and the experiment gives the same result within the experimental errors. Similar selection rules are displayed by the S_c^* gratings in the limit of small sample thickness⁸, and can therefore be considered as "weak selection rules".

REFERENCES

1. R. B. Meyer, Phys. Rev. Lett., **22**, 918 (1969).
2. F. Lonberg and R. B. Meyer, Phys. Rev. Lett., **55**, 718 (1985).
3. J. P. Bobilev and S. A. Pikin, Zh. Eksp. Teor. Fiz., **72**, 369 (1977) [Sov. Phys. JETP, **45**, 195 (1977)].
4. Y. Bobilev, V. G. Chigrinov and S. A. Pikin, J. Phys. (Paris) Colloq., **40**, C3-331 (1979).
5. S. A. Pikin, Structural transformations in liquid crystals (Gordon and Breach, New York, 1991).
6. K. A. Suresh, P. B. Sunil Kumar and G. S. Ranganath, Liq. Cryst., **11**, 73 (1992).
7. J. A. Kosmopoulos and H. M. Zenginoglou, Appl. Opt., **26**, 1714 (1987); H. M. Zenginoglou and J. A. Kosmopoulos, Appl. Opt., **27**, 3898 (1988); Appl. Opt., **28**, 3516 (1989).
8. P. Galatola, C. Oldano and P. B. Sunil Kumar, J. Opt. Soc. Am. A, **11**, 1315 (1994).
9. K. A. Suresh, Yuvaraj Sah, P. B. Sunil Kumar and G. S. Ranganath, Phys. Rev. Lett., **72**, 2863 (1994).
10. P. Galatola, C. Oldano and M. Rajteri, Phys. Rev. E, **49**, 1458 (1994).
11. R. Petit, Electromagnetic theory of gratings (Springer-Verlag, Berlin, 1980).
12. R. V. Johnson and A. R. Tanguay Jr., Opt. Engin., **25**, 235 (1986).
13. K. Rokushima and J. Yamakita, J. Opt Soc Am., **73**, 901 (1983).
14. E. M. Terent'ev and S. A. Pikin, Zh. Eksp. Teor. Fiz., **83**, 1038 (1982).
15. P. G. de Gennes, The physics of liquid crystals (Clarendon Press, Oxford, 1975).